J Biomol NMR (2013) 57:167–178
DOI 10.1007/s10858-013-9777-z

ARTICLE

NMR spectroscopy reveals unexpected structural variation at the protein–protein interface in MHC class I molecules

Monika Beerbaum · Martin Ballaschk · Natalja Erdmann · Christina Schnick · Anne Diehl · Barbara Uchanska-Ziegler · Andreas Ziegler · Peter Schmieder

Received: 7 May 2013 / Accepted: 28 August 2013 / Published online: 5 September 2013

Abstract β_2-Microglobulin (β_2m) is a small, monomorphic protein non-covalently bound to the heavy chain (HC) in polymorphic major histocompatibility complex (MHC) class I molecules. Given the high evolutionary conservation of structural features of β_2m in various MHC molecules as shown by X-ray crystallography, β_2m is often considered as a mere scaffolding protein. Using nuclear magnetic resonance (NMR) spectroscopy, we investigate here whether β_2m residues at the interface to the HC exhibit changes depending on HC polymorphisms and the peptides bound to the complex in solution. First we show that human β_2m can effectively be produced in deuterated form using high-cell-density-fermentation and we employ the NMR resonance assignments obtained for triple-labeled β_2m bound to the HLA-B*27:09 HC to examine the β_2m-HC interface. We then proceed to compare the resonances of β_2m in two minimally distinct subtypes, HLA-B*27:09 and HLA-B*27:05, that are differentially associated with the spondyloarthropathy Ankylosing Spondylitis. Each of these subtypes is complexed with four distinct peptides for which structural information is already available. We find that only the resonances at the β_2m-HC interface show a variation of their chemical shifts between the different complexes. This indicates the existence of an unexpected plasticity that enables β_2m to accommodate changes that depend on HC polymorphism as well as on the bound peptide through subtle structural variations of the protein-protein interface.

Keywords MHC class I · HLA-B27 subtypes · NMR assignment · Protein flexibility · Protein expression · Labeling · β_2-Microglobulin

Abbreviations

OD_{600nm}	Optical density of the culture at 600 nm
MHC	Major histocompatibility complex
HLA	Human leucocyte antigen
β_2m	Beta-2-microglobulin
HC	Heavy chain of an MHC class I molecule
TROSY	Transverse relaxation optimized spectroscopy
HSQC	Heteronuclear single quantum correlation
NMR	Nuclear magnetic resonance
HCDF	High cell density fermentation
BMRB	BioMagResBank

Introduction

The major histocompatibility complex (MHC; in human HLA complex) encodes antigens that play a major role in the immune system of vertebrates. Two types of these molecules (class I and class II, respectively) exert their function by presenting antigenic peptides to either $CD8^+$ or $CD4^+$ T lymphocytes that mediate adaptive immune responses. In addition, the human MHC is associated with almost all autoimmune diseases and several autoinflammatory disorders (Horton et al. 2004). While many of these are connected to HLA class II loci, others are clearly associated with MHC class I alleles, as in the case of the spondyloarthropathy

M. Beerbaum · M. Ballaschk · N. Erdmann · A. Diehl · P. Schmieder (✉)
Leibniz-Institut für Molekulare Pharmakologie (FMP), Robert-Rössle-Str. 10, 13125 Berlin, Germany
e-mail: schmieder@fmp-berlin.de

C. Schnick · B. Uchanska-Ziegler · A. Ziegler
Institut für Immungenetik, Charité-Universitätsmedizin Berlin, Freie Universität Berlin, Thielallee 73, 14195 Berlin, Germany

Ankylosing Spondylitis (AS) which is associated with *HLA-B27* (Brown 2011; Reveille 2012). Over the last decades, the connection of AS to *HLA-B27* has been a field of intense research, but the reason underlying the genetic predisposition is still unknown. Nevertheless, it has been found that individuals with the *HLA-B*27:05* subtype (in short, *B*27:05*) may acquire the disease, while those that are *HLA-B*27:09* (in short, *B*27:09*)-positive do not, although the difference between these two HLA-B27 subtypes is restricted to a single amino acid exchange (Asp116 in *B*27:05* and His116 in *B*27:09*) at the floor of the peptide binding groove (D'Amato et al. 1995). We expect that a comparison of these subtypes using biophysical, biochemical, and functional techniques will eventually shed light on the problem how two minimally distinct histocompatibility antigens can be differentially associated to a multi-factorial disease such as AS (Ziegler et al. 2009).

Major histocompatibility complex class I molecules are cell surface membrane glycoprotein complexes that consist of three components: a highly polymorphic heavy chain (HC), a non-covalently associated light chain, β_2-microglobulin (β_2m), and a peptide of usually 8 to 10 amino acids derived from self- or nonself-proteins (Madden 1995; Rudolph et al. 2006). This extracellular molecular assembly ($M_r \sim 45$ kDa) is anchored to the cell membrane via a single trans-membrane α-helix and a short intracellular part of the HC. The protein complex investigated by X-ray crystallographic or other biophysical techniques consists exclusively of the three extracellular domains of the HC, β_2m, and a peptide.

A wealth of structural and biophysical information on HLA-B27 subtypes has accumulated over the last years, in particular on the subtype pair B*27:05 and B*27:09. While X-ray crystallography has revealed that there are considerable conformational differences between the peptides displayed by the complexes, the structures of the HC and of β_2m, however, are almost indistinguishable (Ziegler et al. 2009). Other methods, while advancing our understanding of the biophysical properties of HLA-B27 molecules, have also not been able to account for the different roles of HLA-B27 subtypes in the pathogenesis of AS, although experiments with B*27:05/human β_2m-transgenic rats have shown that the products of the two transgenes are responsible for AS-like symptoms in the animals (Hammer et al. 1990; Taurog 2009). As an example for the structural organization of MHC class I molecules investigated here, the structure of B*27:09 in complex with the peptide pVIPR is shown in Fig. 1, with the peptide in the canonical conformation (see Table 1).

Apart from elucidating the role of HLA-B27 molecules in AS (Uchanska-Ziegler et al. 2013), we are interested in exploring differences between minimally distinct MHC class I subtypes at atomic resolution in order to obtain a more complete description of the surface that is presented to T-cell receptors. As these experiments rely on the availability of large amounts of labeled, in particular deuterated, proteins, we first describe a high yield, cost-effective production procedure using high-cell density fermentation (HCDF). We then assign the backbone resonances of β_2m in the complex of B*27:09 displaying the self-peptide pVIPR. As chemical shift is a sensitive indicator of structural changes, these resonance assignments serve as the basis to investigate a set of seven further HLA-B27 molecules by analyzing the variability of the amino proton and nitrogen chemical shifts in identical positions. While the overall structures of the different complexes are extremely similar as seen by X-ray crystallography, we demonstrate the existence of structural variability of β_2m

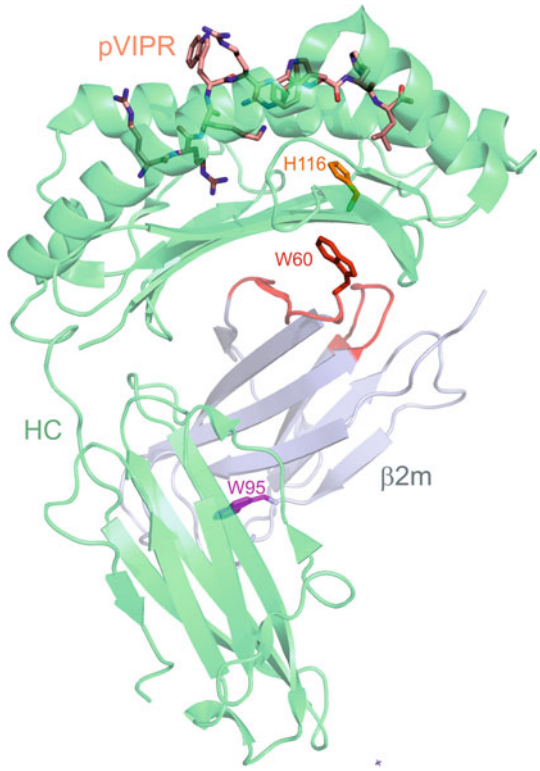

Fig. 1 X-ray structure of one of the HLA-B27 molecules investigated here: the complex consists of B*27:09 (HC), β_2m and the pVIPR peptide. The heavy chain and β_2m are shown as *ribbons* in *green* and *light blue*, respectively, while the peptide is shown as stick representation. Three amino acids of the proteins are shown with their side chains: the two Trp residues that are discussed here (see also Fig. 6) and the polymorphic amino acid 116 (His in B*27:09 and Asp in B*27:05), the only difference between the two subtypes. That part of β_2m which shows chemical shift differences between the eight different complexes investigated here is depicted in *red* (see also Fig. 3 for more detail). It can be seen in the structure that the side chains of the aromatic residues of the peptide (pTrp4 and pTrp7) point away from the bottom of the binding groove. This orientation of aromatic peptide residues is observed in all structures of the complexes discussed here (Ziegler et al. 2009)

Table 1 Properties of the peptides employed in this study

Peptide designation	Sequence	Peptide conformation	
		B*27:09 (pdb-code)	B*27:05 (pdb-code)
pVIPR	RRKWRRWHL	CC (1of2) (Hülsmeyer et al. 2004)	50 % CC, 50 % NC (1ogt) (Hülsmeyer et al. 2004)
TIS	RRLPIFSRL	CC (1w0w) (Hülsmeyer et al. 2005)	CC (1w0v) (Hülsmeyer et al. 2005)
pGR	RRRWHRWRL	CC (3czf) (Ziegler et al. 2009)	2 × NC (2a83) (Rückert et al. 2006)
pLMP2	RRRWRRLTV	CC (1uxw) (Fiorillo et al. 2005)	NC (1uxs) (Fiorillo et al. 2005)

Four peptides are used in the present investigation, whose sequences are given together with their conformation when bound to the HC of one of the HLA-B27 subtypes (*CC* canonical conformation with the middle of the ligand bulging out of the peptide binding groove, *NC* non-canonical conformation in which the middle of the peptide is oriented towards the binding groove). The pdb-code of the structure of the complex and the relevant reference are also provided

around its highly conserved residue Trp60 which is located in the center of the β_2m-HC interface.

Results

Protein production and sample preparation

Since the present investigation concentrated on β_2m, this protein was the only component that had to be labeled for NMR experiments. All peptides were synthesized inhouse by solid-phase procedures and B*27:05 and B*27:09 HC were produced as previously described (Hülsmeyer et al. 2002). The refolding protocol for the formation of the complexes was also carried out using established procedures (Garboczi et al. 1992). The comparison of the chemical shifts for the set of complexes was performed using only ^{15}N labeling of β_2m and the protein was produced as published (Fabian et al. 2008).

For the residue assignments, however, one of the complexes had to be produced utilizing ^{2}H,^{13}C,^{15}N-β_2m. The *E. coli* strain XA90 which has been used for expression of β_2m since several years did not show a sufficient growth and expression behaviour in D_2O-containing medium in shaking flasks with or without adaptation. We therefore decided to establish an expression protocol using HCDF, based on a protocol developed previously (Fiedler et al. 2007). In order to improve the deuteration level water was eliminated from the air used in the fermentation. We did not employ an adaptation of the cells to D_2O, but inoculated the D_2O-based culture with cells collected from a preculture (H_2O-based, not overgrown, 20 °C over night) with a starting OD_{600nm} of 1.2–1.5. The OD_{600nm} dropped during the first hours, but increased significantly afterwards up to a final OD_{600nm} of 12. Cell mass was generated from unlabeled C and N sources up to 1 h before induction, then a feed using labeled material was started. This protocol was used for the production of triple-labeled β_2m that was subsequently incorporated in a complex with the B*27:09 HC and the pVIPR peptide (see Table 1).

Assignment of resonances in β_2m using NMR-spectroscopy

As the first step of the investigation of β_2m in different MHC molecules, an assignment of the backbone resonances in the ^{1}H,^{15}N correlation of complexed β_2m had to be obtained. The experiments to yield spectra for assignment were performed using the B*27:09 subtype and pVIPR, thus consisting of an HC, β_2m and a peptide in the canonical conformation (Table 1), with 276, 100 and 9 amino acids, respectively. Since the molecular weight of the complex (45 kDa) is fairly large for NMR spectroscopy, all experiments were performed as TROSY (Pervushin et al. 1997) versions using a sample in which β_2m was labelled with ^{2}H, ^{13}C and ^{15}N, while the HC and the peptide remained unlabelled. A set of six conventional triple resonance experiments (Cavanagh et al. 1996; Tugarinov et al. 2004) were executed: HNCACB/HN(CO)-CACB and HNCO/HNCACO to obtain two pairs of spectra that could be used for a standard sequential assignment. In addition, an HNCA and an HN(CO)CA were performed using constant-time in the carbon dimension. While these spectra contain less information than those that also contain the shifts of the C_β, their superior resolution was used to resolve overlaps in the other spectra and to check the assignments for consistency. β_2m consists of 100 amino acids; subtracting the 5 proline residues and the amino acid in position 1, it should be possible to assign a total of 94 residues. However, only 91 could be assigned, while signals for three amino acids (His31, Lys58 and Ser88) were undetectable, most likely because they are broadened by conformational exchange. In the case of His31, this assumption is supported by inspection of the X-ray-structure (obtained at 100 K), which shows two conformations for this residue in all eight structures of the complexes

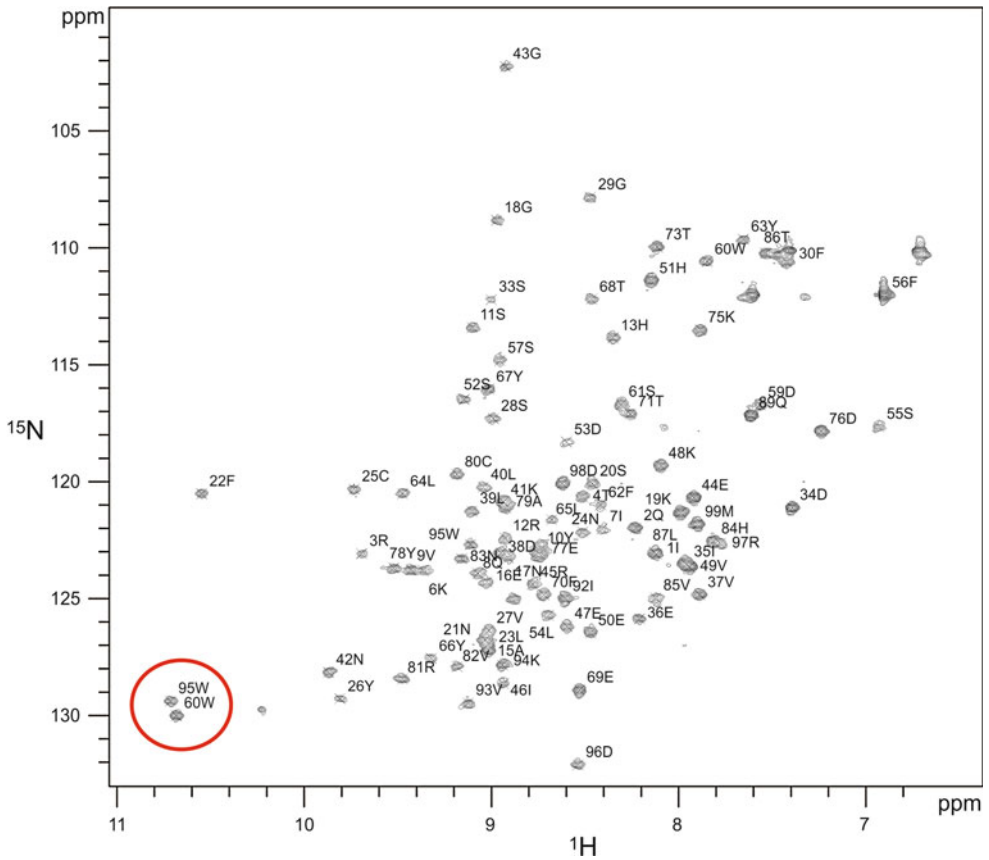

Fig. 2 Assignment of signals for β_2m in complex with the B*27:09 HC and the pVIPR peptide. The $^{1}H,^{15}N$-TROSY spectrum of β_2m in complex with B*27:09 and pVIPR shows signals exclusively from β_2m since only this protein was labelled with ^{15}N. All $^{1}H,^{15}N$-correlations except those of His31, Lys58 and Ser88 are visible and could be assigned. The resonances in the *red circle* are those of the $H^{N\varepsilon}/N^{\varepsilon}$ pair in the two tryptophan side chains which are more closely inspected in Fig. 6

investigated here. Interestingly, an X-ray-structure determined at room temperature shows only one conformation for this residue (B. Loll, personal communication). The full $^{1}H,^{15}N$ correlation with assignments is shown in Fig. 2.

Transfer of resonance assignments between individual MHC molecules

Since chemical shift is a sensitive indicator of changes in structure, we decided to compare the $^{1}H,^{15}N$ correlations of β_2m in a set of eight different complexes, using the two HC mentioned above and the three self-peptides pVIPR, TIS, and pGR as well as the viral peptide pLMP2 (Table 1). High-resolution structures obtained by X-ray crystallography are available for all eight complexes (see Table 1 for pdb-codes and references) and indicate that the structure of β_2m is invariable. We expected to be able to transfer the assignment of pVIPR-B*27:09 to all other complexes and this turned out to be possible. A comparison of a region of the $^{1}H,^{15}N$ correlation of pVIPR-B*27:09 and pVIPR-B*27:05 is shown in Fig. 3. Given that spectra were recorded using almost identical sample conditions, it is not surprising that most of the peaks were found in identical positions, since the structures of the two HC subtypes and β_2m appear to be nearly indistinguishable. The different conformations (canonical or non-canonical) of the peptides as determined by X-ray crystallography (Table 1) did not have a systematic influence on the chemical shifts observed for β_2m residues. Some of the peaks, however, were shifted slightly, indicating subtle structural differences between the individual complexes. All assignments were deposited in the BMRB, the accession codes are given in Table 2.

Comparative analyses of HLA-B27 subtypes complexed to four peptides

Similar variations as seen in Fig. 3 could be found when we compared all eight complexes with each other. To analyse the variability of the chemical shifts in a systematic manner, an average peak position was calculated from the shifts of all four spectra of each subtype. To compare the two subtypes, we calculated the difference between the two average spectra (Fig. 4a). In addition, the average difference between the average peak and the peaks in the

Table 2 BMRB accession codes for the assignment of β_2m

Peptide	Sequence	BMRB code for β_2m assignment	
		B*27:09	B*27:05
pVIPR	RRKWRRWHL	19113	19120
TIS	RRLPIFSRL	19116	19121
pGR	RRRWHRWRL	19119	19123
pLMP2	RRRWRRLTV	19118	19122

individual spectra was calculated for each of the two subtypes (Fig. 4b, c). Three regions of β_2m show non-negligible variations in the chemical shifts in a comparison of the two subtypes, the most prominent being the region containing Asp53, Lys58 and Trp60. These residues belong to a loop region that has already been identified as being in slow conformational exchange in free β_2m (Okon et al. 1992; Esposito et al. 2008; Eichner et al. 2011; Hee et al. 2013). In addition, two other regions, namely the N-terminus and another loop that is contacting the HC (the region around His31), show enhanced variations in the chemical shift. Within a given subtype, the variability of the chemical shifts was less pronounced, but again was largest in two of the three areas that differ most between the subtypes, with only the N-terminal residues appearing unaffected. A graphical representation of the variability found between subtypes is shown in Fig. 3b.

Analysis of the chemical shift of signals from tryptophan residues in β_2m

In order to further investigate the region's variability where it is most prominent, we compared the chemical shifts of the HNE1 protons of tryptophan (red circle in Fig. 2). β_2m contains two Trp residues (see Fig. 1): Trp95 is located in the core of the structure, while Trp60 resides on the outside of free β_2m and within an MHC class I molecule in highly conserved contacts with residues of the HC. It forms hydrogen bonds with Gln96 ($Trp60^{O}$–$Gln96^{NE2}$) and Asp122 ($Trp60^{NE1}$–$Asp122^{OD1/2}$) as well as a universally retained van der Waals contact with Ala117 of an HC (Hee et al. 2013) as shown in Fig. 5. All three HC residues are highly conserved and constitute part of the floor of the peptide binding groove, in the immediate vicinity of residue 116 which exhibits the highest degree of polymorphism of any HC residue in HLA-B antigens (Reche and Reinherz 2003). If the loop in which Trp60 is positioned did in fact exhibit structural variability in an HLA-B27 subtype- and peptide-dependent fashion, one would expect that the position of the $Trp60^{NE1}$-bound proton were also

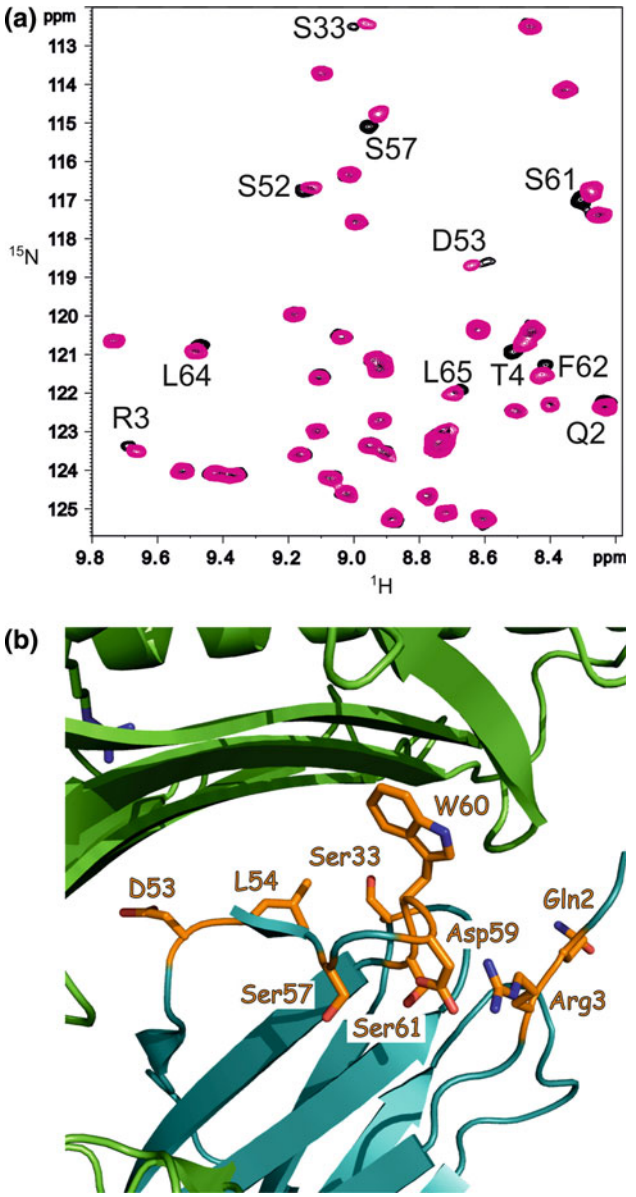

Fig. 3 Transfer of assignment between HLA-B27 subtypes. **a** A superposition of two identical regions from the ^{1}H,^{15}N-HSQC spectra of pVIPR-B*27:09 and pVIPR-B*27:05 is shown, both with only β_2m labelled with ^{15}N. While the majority of the resonances are in identical positions in the spectra, several signals exhibit a slight shift. Some signals (e.g. S33 and D53) also exhibit broad lines due to conformational exchange. Differences in chemical shifts can also be seen between complexes of a given HLA-B27 subtype bound to different peptides. A full analysis of the shifts is shown in Fig. 4. **b** Graphical representation of the chemical shift variability. The amino acids whose ^{1}H,^{15}N correlation *peaks* show a difference of more than 0.025 ppm between the averaged subtype spectra (Fig. 4a) are shown with side chains (*orange*). The backbone of the HC is depicted in *green*, that of β_2m in *light blue*. Clearly, only residues at the interface to the HC show significant variations of the chemical shift. His31 and Lys58 are missing from the figure since they do not produce a signal in the spectrum and thus cannot have a value for shift variability

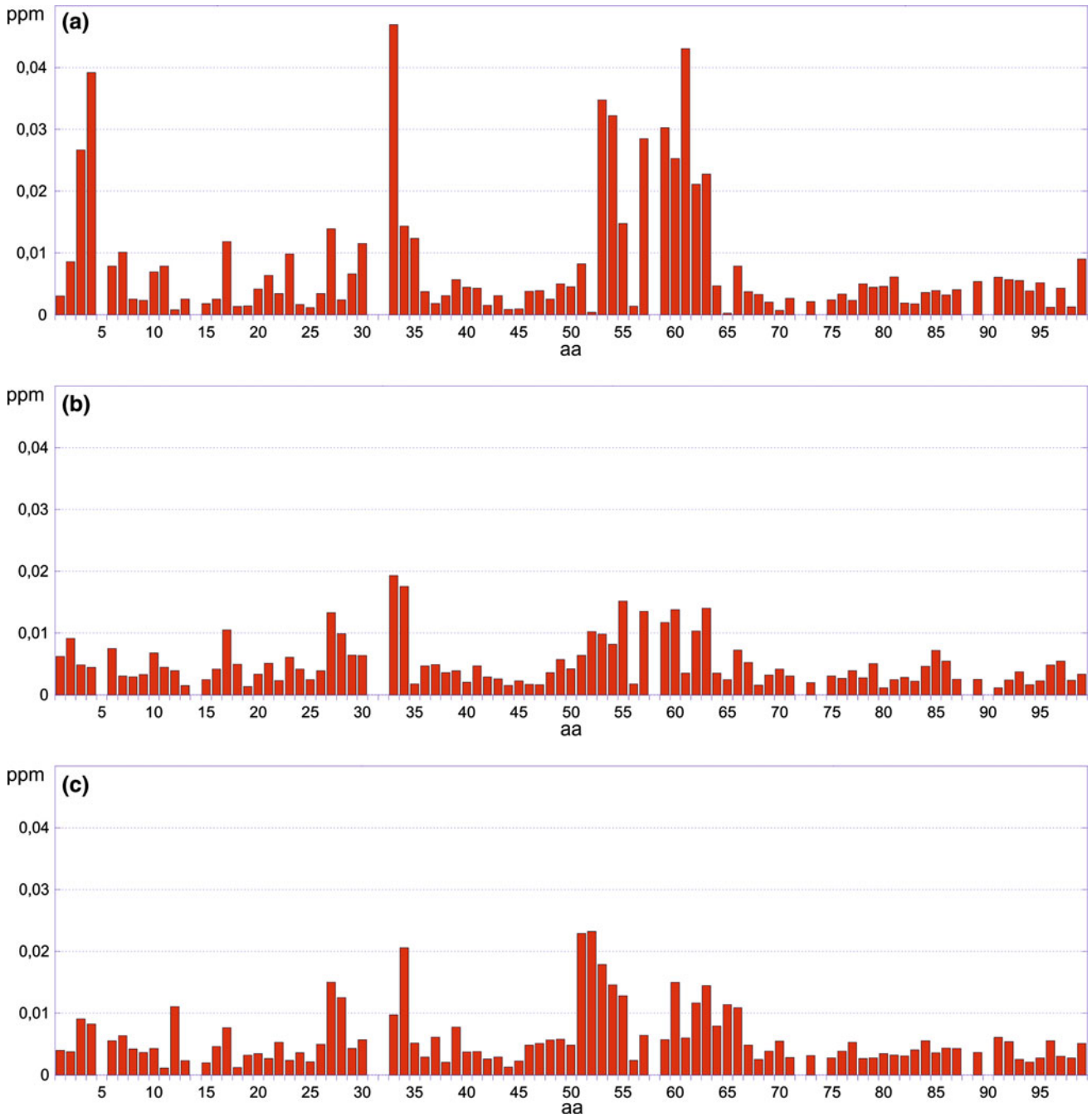

Fig. 4 Variability of chemical shifts of β_2m residues in a set of eight MHC class I molecules. Two HLA-B27 subtypes in complex with four different peptides (see Table 1) are compared. The deviation of the chemical shifts is always calculated using the formula shift = sqrt[$(\Delta\delta(^1H))^2 + (\Delta\delta(^{15}N)/10)^2$] ($\Delta\delta$ is the difference in chemical shift in the respective dimensions). **a** The differences between the chemical shifts of the average spectra of both subtypes (obtained by creating an averaged peak position from all four ^1H,^{15}N correlations for each amino acid) is shown. Three regions reveal the highest degree of variability (see also Fig. 3b): the N-terminus, the region around His31 and the region around Asp53 and Trp60. **b** Chemical shift variation within B*27:09, where the average deviation between an individual spectrum and the average spectrum is shown for each amino acid. Only small variation around His31 and the region around Asp53 and Trp60 is visible. **c** Chemical shift variation within B*27:05, with the average deviation between an individual spectrum and the average spectrum shown for each amino acid. The variability is comparable to that in B*27:09

characterized by a variation in chemical shift, most likely due to a variation in the length of the hydrogen bond to Asp122. This is indeed what we observed (Fig. 6). While the resonance of Trp95 does not show any variation in chemical shift, thus serving as an ideal internal control, there are distinct resonance signals for the Trp60 residue in

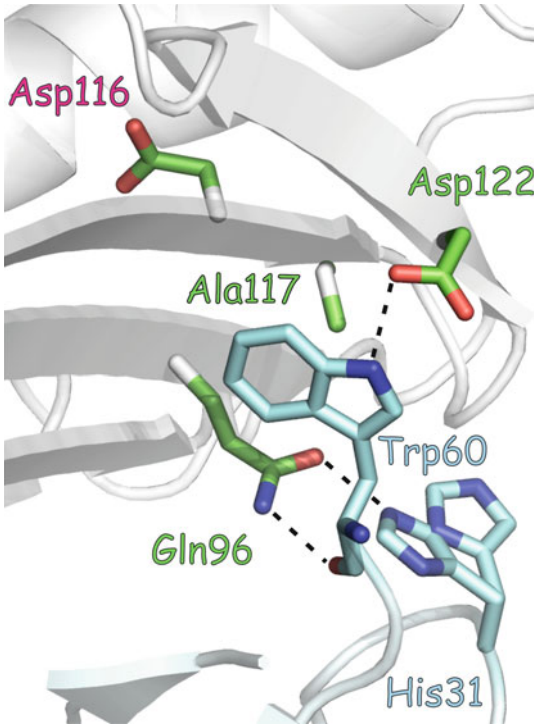

Fig. 5 Crucial β_2m-HC interface residues in the structure of an MHC molecule. The HC-β_2m interface of the TIS-B*27:05 complex is shown (similar contacts can be found in the other seven complexes). The backbone of the HC is shown in *light grey*, that of β_2m in *grey*. Highly conserved amino acids are shown with their side chains: Gln96, Ala117 and Asp122 of the HC, Trp60 and His31 in β_2m. Note the double conformation of His31 which is observed at 100 K. The polymorphic residue 116 (Asp in B*27:05, His in B*27:09) is indicated in *red script*. The three amino acids of the HC that contact β_2m residues are part of the β-strands around the polymorphic amino acid 116 and form a highly conserved interface (Hee et al. 2013) with amino acids in β_2m. Differences in structure and dynamics of the HC that are due either to HC polymorphisms or to different peptides are relayed via this interface. Apparently, the β_2m-side of the interface needs to be flexible to accommodate these differences. The figure was created using PyMol (DeLano 2002)

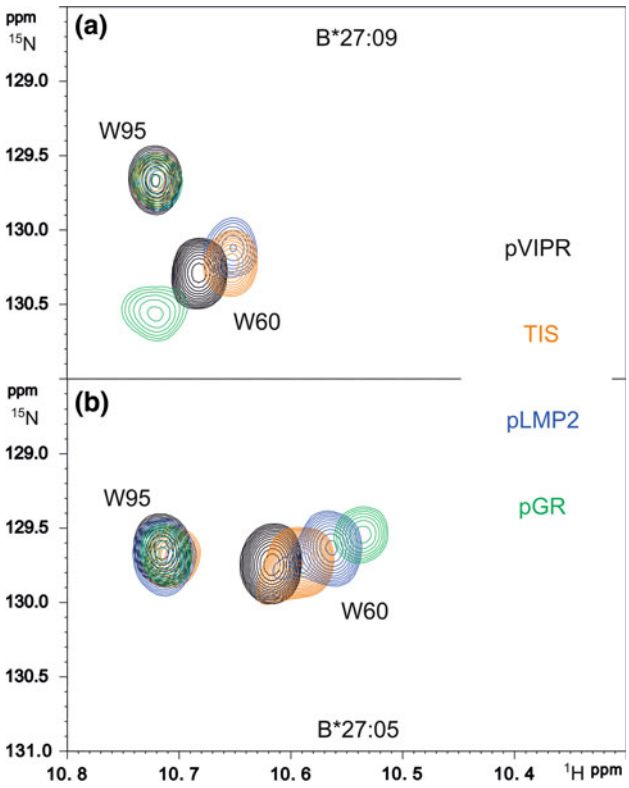

Fig. 6 Subtype- and peptide-dependent variation of the chemical shift of β_2m-Trp60. To assess the variation of the peak position for the $H^{N\varepsilon}/N^{\varepsilon}$ pair of Trp60 in β_2m complexed with B*27:09 or B*27:05 and different peptides, only the region of the $H^{N\varepsilon}/N^{\varepsilon}$ pairs in the spectra is shown (*red circle* in Fig. 2). The resonances of the same pair of Trp95 remain in an identical position in each spectrum, independent of the HC or the peptide. In contrast, the $H^{N\varepsilon}/N^{\varepsilon}$ pair of Trp60 shows two groups of resonances depending on the HLA-B27 subtype and a further variation within each of these two groups that depends on the bound peptide

each of the eight peptide-HLA-B27 complexes investigated here. Therefore, these signals are not only distinguishable for a given HLA-B27 subtype, but are also in characteristic positions within the spectra for each of the four peptides employed here, indicating structural variability of the Trp60 side chain.

Discussion

For a full understanding of the interaction between MHC class I molecules and their protein ligands such as a TCR, structural information at atomic resolution is absolutely essential. An extensive set of high-resolution structures has become available over the last 25 years, both of the individual components (Bjorkman et al. 1987; Madden et al. 1992; Madden 1995; Ziegler et al. 2009) as well as of MHC-TCR complexes (Rudolph et al. 2006; Baker et al. 2012). This information has almost exclusively been obtained through X-ray crystallography and has allowed addressing many questions, not only regarding the details of the interaction, but also as far as important immunological concepts are concerned such as cross-reactivity and recognition of self-antigens by TCR (Yin and Mariuzza 2009; Gras et al. 2011). It has, however, also become clear that it will not be sufficient to take only rigid structures into account, and that information on subtle structural changes and on the mobility within the individual complexes will also be required (Baker et al. 2012). Attempts have been made to obtain such data by comparing X-ray structures (Garcia et al. 1998; Reiser et al. 2003; Kjer-Nielsen et al. 2003; Borbulevych et al. 2009; Kumar et al. 2009) or by employing molecular dynamics (MD) simulations (Rognan et al. 1994; Michielin and Karplus 2002; Wan et al. 2004;

Zacharias and Springer 2004; Fabian et al. 2008; Narzi et al. 2012), as well as IR spectroscopic (Fabian et al. 2008, 2010, 2011) and mass spectroscopic procedures (Hodkinson et al. 2009; Hawse et al. 2012).

A very important additional method, however, that can in principle provide a very detailed picture of the mobility of proteins and protein complexes at atomic resolution is NMR spectroscopy, which also permits the detection of motions on a variety of time scales (Mittermaier and Kay 2009; Mittermaier and Kay 2006). For MHC molecules or TCR, this technique has only rarely been applied (Hare et al. 1999; Varani et al. 2007; Insaidoo et al. 2009; Günther et al. 2010), but with recent advances regarding the size of the molecules that can be assigned and analyzed (Tugarinov et al. 2004), MHC class I molecules are now well within the reach of this method. However, when addressing the influence of HC polymorphism and different peptides on the spectroscopic properties of MHC molecules, samples of at least two HLA-subtypes, each equipped with different peptides, need to be produced (Pöhlmann et al. 2004; Winkler et al. 2007; Fabian et al. 2008, 2010, 2011).

To obtain information about structure and dynamics from NMR spectroscopy, the proteins have to be labeled with NMR-active isotopes and—given the size of the complexes—also deuterated to improve the relaxation properties and to make full use of the TROSY-type NMR experiments. Procedures to express deuterated proteins are still under discussion since D_2O has serious effects on biological molecules and consequently on living cells (Kushner et al. 1999; Giovanni 1961). There are two different approaches to grow *E. coli* cells in deuterated medium. One favours the stepwise adaptation of the cells to higher D_2O concentrations (Cohen et al. 2010; Paliy et al. 2003), the other prefers the direct inoculation into medium containing 100 % D_2O (Leiting et al. 1998; Zhu et al. 2012). According to information from the deuteration lab in Grenoble (http://jra7.neutron-eu.net/FILES/D2.1_report_EMBL.pdf) the best strategy depends on the type of *E. coli* strain. B-type strains (BL21 and its derivatives) have been characterized as deuterium-tolerant in contrast to most of the K12 strains which have to be adapted via increasing D_2O content. In line with that we obtained best expression for 100 % deuterated proteins with BL21-derivatives without adaption to D_2O.

There are several advantages connected with the use of HCDF: the first is the efficient use of isotopes, with the expression of triple labeled kinesin in HCDF compared to a shaking culture performed in our laboratory (J. Zapke, personal communication) serving as an example: we found a tenfold yield per l, using a fivefold amount of ^{13}C and ^{15}N source resulting in half the costs for these two isotopes. More importantly, the amount of D_2O can be reduced to one tenth. Another advantage of HCDF is the possibility to eliminate H_2O from air to obtain particularly high deuteration levels [see for example (Röben et al. 2010)]. On the other side a drawback of HCDF is the requirement for a magnetic stirrer, which can lead to disintegration of cells. In case of target proteins coded on plasmids with Ampicillin resistance β-lactamase is thereby set free into the medium and reduces the selection pressure, resulting in a decrease in specific product formation. In those cases we have successfully used the concentration method (Marley et al. 2001): here the culture is grown on H_2O containing LB medium, cells are collected in the middle of the log phase and resuspended in half of the volume of D_2O based M9-medium (K. Rehbein, personal communication). Another approach that is not as efficient as HCDF but also makes more effective use of the isotopes is the expression in Ultra Yield Flasks (Thomson). Moreover, as in HCDF the oxygen supply is improved in those flasks as compared to standard flasks.

It can be expected that the dynamic features of the complexes that will be most important for an understanding of TCR binding are those of the peptide and the HC, in particular its α1- and α2-domains. Nevertheless, it should be kept in mind that an MHC molecule is an entity in which β2 m, even if it does not contact a TCR, is still part of the overall complex and is thus likely to participate in the dynamics of the entire molecule (Hawse et al. 2012). In addition, this component of the complex will also be in contact with the CD8 molecule, an integral part of the recognition assembly. As a first step with regard to a comparative analysis of all components of MHC class I molecules, we employed β_2m, which exhibits a $^{1}H,^{15}N$ correlation with hardly any overlap (Fig. 2). As the structures of β_2m in all complexes investigated here are virtually indistinguishable (see the references provided in Table 1) and since all spectra were recorded with freshly prepared samples at the same temperature, field strength, and concentration, any variation of chemical shifts indicates a subtle change in structure and thus points toward plasticity within the protein. Changes in chemical shift can also be caused by effects of anisotropy, in particular when aromatic side chains are present or in cases of a variation of the number of aromatic residues between bound peptides as in MHC class I molecules. As can be seen from Fig. 1, however, aromatic peptide side chains of the complexes investigated here point outward and thus away from the interface. The other variation is that of residue 116, the micro-polymorphism distinguishing B*27:05 and B*27:09. This residue is also pointing away from the interface but is still close to the side chain of Trp60 (see below).

We observe that the differences between the two HLA-B27 subtypes complexed with four peptides are on one hand sufficiently small to transfer the assignment obtained for the pVIPR-B*27:09 complex to the others, but on the

other hand sufficiently large to find significant differences (Fig. 3). We have previously analyzed the distinction between β_2m free in solution and when bound within the pVIPR-B*27:09 complex (Hee et al. 2013), revealing that four regions of β_2m (the N-terminus, residues 30–33, residues 51–63, as well as residues 88–89) show increased dynamics in free form. Upon binding to the HC, the protein rigidifies, but still exhibits enhanced mobility in the case of three regions of the protein, with three residues that could not be assigned due to conformational exchange (His31, Lys58, Ser88). Here we demonstrate that the remaining plasticity in these regions leads to subtle structural differences between very closely related MHC class I molecules (Figs. 3, 4).

IR spectroscopic experiments as well as MD simulations have previously been performed on the same complexes. Both types of analysis showed that larger fluctuations exist in the peptide binding groove of B*27:05 than in that of B*27:09 (Fabian et al. 2008, 2010, 2011; Narzi et al. 2012). According to these studies, HC flexibility must be regarded as an HC-intrinsic, MHC polymorphism-dependent property. We have already suggested a molecular explanation for the finding that the buried HC residue 116 can exert a pronounced effect on the dynamics of the two α-helices of the molecule, although there are no direct contacts between the floor and the rims of the peptide binding groove, respectively. Our reasoning involves interactions between this polymorphic residue, the water cushion below the peptide, and universally preserved contacts between the main chain of a peptide and residues belonging to each of the α-helices (Fabian et al. 2010, 2011). In addition, electrostatic attraction between the HC residues Asp77 and His116 (B*27:09) or repulsion (Asp77 and Asp116 in B27:05) might influence the mobility of the a1-helix, as suggested by MD simulations (Narzi et al. 2012). Similarly, it is likely that the structure of β_2m has to change slightly to accommodate distinct HC structures via a conserved network of contacts between highly conserved HC residues (Gln96, Ala117, and Asp122) and equally conserved β_2m amino acids (His31 and Trp60) (Fig. 5). These HC residues are either next (Ala 117) to the polymorphic HC residue 116 or in close vicinity, i.e. on neighboring β-strands (Gln96, Asp122).

Changes in the spectrum are particularly pronounced for the side chain of Trp60, an evolutionarily retained (Hee et al. 2013) key residue in β_2m (Figs. 1, 6). Remarkably, differences are not only evident between the two HLA-B27 subtypes, but are also obvious within a given subtype, dependent on which of the four peptides is bound. The variation between the peptides and the difference between minimally distinct HC and peptides complexed with a given subtype cannot be explained with effects of anisotropy alone. It is far more likely that a subtle variation in structure is present, in particular since the chemical shift observed here is sensitive to the length of hydrogen bonds between Trp60 and residues of the HC. It seems plausible that direct contacts to β_2m-Trp60 through the HC residues Gln96 and Asp122 (via H-bonds) as well as Ala117 (via van der Waals contacts) contributes to the transfer of changes in the HC to β_2m. The β_2m region which we find to exhibit the most pronounced alterations and that is likely to be influenced particularly by exchanges of residues in the peptide binding groove, either due to HC polymorphisms or variation of the peptide, is that which is contacted also by a CD8 molecule in the target/effector cell complex (Trp60, Lys58) (Gao et al. 1997, Shi et al. 2011).

Conclusions

Apart from providing an efficient protocol for the production of large quantities of the protein components of MHC class I molecules labelled with NMR-relevant isotopes, the most important result of our study is the realization that MHC polymorphisms can influence not only the structure of the HC or the conformation of the binding groove, but also that of β_2m in MHC class I molecules. The successful transfer of the assignment of β_2m in the pVIPR-B*27:09 complex to β_2m in seven further B*27:05 and B*27:09 complexes reveals that certain parts of the protein exhibit a plasticity that results in subtle structural adjustments in the various complexes. This influence is especially notable in the case of β_2m-Trp60, whose structure and contact to the heavy chain depends not only on the HC of the HLA-B27 subtype with which β_2m is complexed, but even on as yet unknown properties of a bound peptide. Our work lays the foundations for a quantification of protein mobility in MHC class I complexes and a full analysis of the relaxation times. It is important to note, however, that a complete investigation of the dynamics of the protein-protein interface in MHC molecules will require the study of both β_2m and the HC and would therefore go beyond the scope of this paper. Work to obtain assignments for HC residues and to perform a full dynamic analysis of both sides of the interface is in progress in our laboratory. Such studies will eventually contribute to shed light on the importance of protein dynamics for recognition processes in immune responses, both physiological as well as pathological.

Materials and methods

Production of $^{2}H,^{13}C,^{15}N$-β_2-microglobulin

Triple-labeled β_2m was produced by HCDF (DASGIP Jülich, Germany): a pHN1-based construct (MacFerrin

et al. 1990) of human β_2m was used to transform *E. coli* XA 90. 400 µl of an overday preculture grown in 4 ml LB medium at 37 °C with 300 µg/ml carbenicillin (a fivefold concentration of antibiotics compared to the standard is typically employed in every step of the cultivation) were used to inoculate an overnight culture of 400 ml at 20 °C in the same medium. Next day the cells were collected by centrifugation at 5,000*g* and washed with 150 mM NaCl in D_2O. The pellet was finally resuspended in 100 ml of 150 mM NaCl in D_2O. 20 ml were used to inoculate a 250 ml HCDF. The batch medium was 99.8 % D_2O-based minimal medium (twofold M9 salts, trace elements, 2 mM $MgSO_4$, 0.3 mM $CaCl_2$, 3 mg/l thiamin and biotin) with unlabeled glucose (8 g/l) and NH_4Cl (2 g/l). The D_2O-based expression feed (15 ml) contained fivefold M9 salts, trace elements, fivefold thiamin and biotin, 4 g d_7-^{13}C-glucose and 1 g ^{15}N-NH_4Cl. The pH was automatically adjusted to 7.5 by adding 2 M NaOD. The stirrer speed was fixed to 500 rpm at levels of dissolved oxygen above 30 % and increased slowly and automatically up to 1,000 rpm when the level dropped below 30 %. The air consumed in the fermentation was dried using a 1.3 kg column of molecular sieve 3A (AppliChem). The temperature decreased from 37 to 22 °C at the beginning of the labeled expression feed, triggered by the increase of oxygen dissolved in the medium above 60 % due to the total exhaustion of carbon and nitrogen sources in the batch fluid. The labeled expression feed ran over 15 h with 1 ml per h. The induction feed consisting of 5 ml 1M isopropyl-β-D-thiogalactopyranoside in D_2O began 1 h after the expression feed and was applied at 40 ml/h. At the end of the fermentation, the culture was cooled to 12 °C and left for harvesting on the next day. Typically an OD_{600nm} of 12 is reached, corresponding to about 37 g of wet biomass from 1 l of culture.

Production of the complexes

All further procedures for the production of the heterotrimeric MHC class I molecules have previously been described: The production of ^{15}N-labeled β_2m, the purification of β_2m from inclusion bodies, the production of *B*27:05* and *B*27:09* HC as well as the reconstitution of the components to yield heterotrimeric complexes (Garboczi et al. 1992; Hülsmeyer et al. 2002; Fabian et al. 2008). Four peptides (pVIPR, derived from vasoactive intestinal peptide type 1 receptor; TIS, derived from epidermal growth factor response factor 1; pGR, derived from glucagon receptor and pLMP2, derived from latent membrane protein 2 of Epstein–Barr virus) were employed for the reconstitutions. The origin of the peptides, their sequences and conformations within the B*27:05 and B*27:09 binding grooves (canonical or non-canonical), as well as the respective reference are given in Table 1. An overview regarding structural and thermodynamic features of these complexes is provided by Ziegler and co-workers (Ziegler et al. 2009).

NMR-spectroscopy

All samples were produced with β_2m labelled for NMR spectroscopy (^{2}H, ^{13}C, ^{15}N for the assignment, ^{15}N for the comparison of chemical shifts). The buffer used for NMR spectroscopy contained 150 mM NaCl and 10 mM phosphate, pH 7.5. All NMR spectra used in the assignment procedure were recorded at 310 K on AV600 Bruker spectrometers (600 MHz ^{1}H frequency). The sample contained triple labelled β_2m and had a concentration of 8.5 mg/ml. The HNCACO was recorded using a TXI cryoprobe equipped with a self-shielding z-gradient, while all other spectra were measured using a TCI cryoprobe, also equipped with a self-shielding z-gradient. The following parameters were used for the experiments: 2D TROSY: 8 scans, data size 512(^{1}H)*256(^{15}N) complex points, $t_{Hmax} = 51.2$ ms, $t_{Nmax} = 85.0$ ms; HNCACB and HNCOCACB 32 scans, data size 512(^{1}H)*40(^{15}N) *48(^{13}C) complex points, $t_{Hmax} = 51.2$ ms, $t_{Nmax} = 13.3$ ms, $t_{Cmax} = 4.8$ ms; constant time HNCA 16 scans, data size 512(^{1}H)*48(^{15}N) *96(^{13}C) complex points, constant time delay (^{13}C) = 27 ms, $t_{Hmax} = 51.2$ ms, $t_{Nmax} = 15.9$ ms, $t_{Cmax} = 19.2$ ms; constant time HNCOCA 16 scans, data size 512(^{1}H)*48(^{15}N) *100(^{13}C) complex points, constant time delay (^{13}C) = 27 ms, $t_{Hmax} = 51.2$ ms, $t_{Nmax} = 15.9$ ms, $t_{Cmax} = 20.0$ ms; HNCACO 48 scans, data size 512(^{1}H)*40(^{15}N) *31(^{13}C) complex points, $t_{Hmax} = 51.2$ ms, $t_{Nmax} = 13.3$ ms, $t_{Cmax} = 12.4$ ms; HNCO 8 scans, data size 512(^{1}H)*48(^{15}N) *48(^{13}C) complex points, $t_{Hmax} = 51.2$ ms, $t_{Nmax} = 15.9$ ms, $t_{Cmax} = 19.2$ ms. All 3Ds were executed as TROSY versions. Recycle delays of 1.3 s were used.

The spectra for the comparison of β_2m in complex with different peptides and different HC subtypes were recorded at 310 K on a AV750 Bruker spectrometer (750 MHz ^{1}H frequency) using a TCI cryo probe. The following parameters were used for the HSQCs: 16 scans, data size 512(^{1}H)*128(^{15}N) complex points, $t_{Hmax} = 41.0$ ms, $t_{Nmax} = 33.8$ ms.

In all cases, processing was performed using topspin 2.1 (Bruker Biospin, Karlsruhe, Germany). The processed data were first converted to UCSF-format (Goddard and Kneller 2004) and subsequently transferred to CCPN (Vranken et al. 2005) for assignment.

Acknowledgments We thank Dr. B. Loll (Freie Universität Berlin) for providing us with unpublished information on β_2m residues in an X-ray structure obtained at room temperature and Dr. M. Dorn for

help with improving the HCDF. Support from the Leibniz-Institut für Molekulare Pharmakologie (FMP) is gratefully acknowledged. The work was funded by the Deutsche Forschungsgemeinschaft (SCHM880/9-1, UC8/2-1).

References

Baker BM, Scott DR, Blevins SJ, Hawse WF (2012) Structural and dynamic control of T-cell receptor specificity, cross-reactivity, and binding mechanism. Immunol Rev 250:10–31

Bjorkman PJ, Saper MA, Samraoui B, Bennett WS, Strominger JL, Wiley DC (1987) Structure of the human class I histocompatibility antigen, HLA-A2. Nature 329:506–512

Borbulevych OY, Piepenbrink KH, Gloor BE, Scott DR, Sommese RF, Cole DK, Sewell AK, Baker BM (2009) T cell receptor cross-reactivity directed by antigen-dependent tuning of peptide-MHC molecular flexibility. Immunity 31:885–896

Brown MA (2011) Progress in the genetics of ankylosing spondylitis. Brief Funct Genomics 10:249–257

Cavanagh J, Palmer AG III, Skelton NJ (1996) Protein NMR spectroscopy, principles and practice. Academic Press, San Diego

Cohen LS, Becker JM, Naider F (2010) Biosynthesis of peptide fragments of eukaryotic GPCRs in *Escherichia coli* by directing expression into inclusion bodies. J Pept Sci 16:213–218

D'Amato M, Fiorillo MT, Carcassi C, Mathieu A, Zuccarelli A, Bitti PP, Tosi R, Sorrentino R (1995) Relevance of residue 116 of HLA-B27 in determining susceptibility to ankylosing spondylitis. Eur J Immunol 25:3199–3201

DeLano WL (2002) The PyMOL Molecular Graphics System. San Carlos, CA, DeLano Scientific

Eichner T, Kalverda AP, Thompson GS, Homans SW, Radford SE (2011) Conformational conversion during amyloid formation at atomic resolution. Mol Cell 41:161–172

Esposito G, Ricagno S, Corazza A, Rennella E, Gumral D, Mimmi MC, Betto E, Pucillo CE, Fogolari F, Viglino P, Raimondi S, Giorgetti S, Bolognesi B, Merlini G, Stoppini M, Bolognesi M, Bellotti V (2008) The controlling roles of Trp60 and Trp95 in beta2-microglobulin function, folding and amyloid aggregation properties. J Mol Biol 378:887–897

Fabian H, Huser H, Narzi D, Misselwitz R, Loll B, Ziegler A, Böckmann RA, Uchanska-Ziegler B, Naumann D (2008) HLA-B27 subtypes differentially associated with disease exhibit conformational differences in solution. J Mol Biol 376:798–810

Fabian H, Huser H, Loll B, Ziegler A, Naumann D, Uchanska-Ziegler B (2010) HLA-B27 heavy chains distinguished by a micropolymorphism exhibit differential flexibility. Arthritis Rheum 62:978–987

Fabian H, Loll B, Huser H, Naumann D, Uchanska-Ziegler B, Ziegler A (2011) Influence of inflammation-related changes on conformational characteristics of HLA-B27 subtypes as detected by IR spectroscopy. FEBS J 278:1713–1727

Fiedler S, Knocke C, Vogt J, Oschkinat H, Diehl A (2007) HCDF as a protein labeling methodology. Genet Eng Biotechnol News 27. http://www.genengnews.com/gen-articles/hcdf-as-a-protein-labeling-methodology/2090/

Fiorillo MT, Rückert C, Hülsmeyer M, Sorrentino R, Saenger W, Ziegler A, Uchanska-Ziegler B (2005) Allele-dependent similarity between viral and self-peptide presentation by HLA-B27 subtypes. J Biol Chem 280:2962–2971

Gao GF, Tormo J, Gerth UC, Wyer JR, McMichael AJ, Stuart DI, Bell JI, Jones EY, Jakobsen BK (1997) Crystal structure of the complex between human CD8alpha (alpha) and HLA-A2. Nature 387:630–634

Garboczi DN, Hung DT, Wiley DC (1992) HLA-A2-peptide complexes: refolding and crystallization of molecules expressed in *Escherichia coli* and complexed with single antigenic peptides. Proc Natl Acad Sci USA 89:3429–3433

Garcia KC, Degano M, Pease LR, Huang M, Peterson PA, Teyton L, Wilson IA (1998) Structural basis of plasticity in T cell receptor recognition of a self peptide–MHC antigen. Science 279:1166–1172

Giovanni R (1961) The effects of deuterium oxide on bacteria. Mol Gen Genet 402:389–402

Goddard TD, Kneller DG (2004) SPARKY 3. University of California, San Francisco

Gras S, Kjer-Nielsen L, Chen Z, Rossjohn J, McCluskey J (2011) The structural bases of direct T-cell allorecognition: implications for T-cell-mediated transplant rejection. Immunol Cell Biol 89:388–395

Günther S, Schlundt A, Sticht J, Roske Y, Heinemann U, Wiesmüller KH, Jung G, Falk K, Rotzschke O, Freund C (2010) Bidirectional binding of invariant chain peptides to an MHC class II molecule. Proc Natl Acad Sci USA 107:22219–22224

Hammer RE, Maika SD, Richardson JA, Tang JP, Taurog JD (1990) Spontaneous inflammatory disease in transgenic rats expressing HLA-B27 and human beta 2m: an animal model of HLA-B27-associated human disorders. Cell 63:1099–1112

Hare BJ, Wyss DF, Osburne MS, Kern PS, Reinherz EL, Wagner G (1999) Structure, specificity and CDR mobility of a class II restricted single-chain T-cell receptor. Nat Struct Biol 6:574–581

Hawse WF, Champion MM, Joyce MV, Hellman LM, Hossain M, Ryan V, Pierce BG, Weng Z, Baker BM (2012) Cutting edge: evidence for a dynamically driven T cell signaling mechanism. J Immunol 188:5819–5823

Hee CS, Beerbaum M, Loll B, Ballaschk M, Schmieder P, Uchanska-Ziegler B, Ziegler A (2013) Dynamics of free versus complexed beta2-microglobulin and the evolution of interfaces in MHC class I molecules. Immunogenetics 65:157–172

Hodkinson JP, Jahn TR, Radford SE, Ashcroft AE (2009) HDX-ESI-MS reveals enhanced conformational dynamics of the amyloidogenic protein beta(2)-microglobulin upon release from the MHC-1. J Am Soc Mass Spectrom 20:278–286

Horton R, Wilming L, Rand V, Lovering RC, Bruford EA, Khodiyar VK, Lush MJ, Povey S, Talbot CC Jr, Wright MW, Wain HM, Trowsdale J, Ziegler A, Beck S (2004) Gene map of the extended human MHC. Nat Rev Genetics 5:889–899

Hülsmeyer M, Hillig RC, Volz A, Ruhl M, Schröder W, Saenger W, Ziegler A, Uchanska-Ziegler B (2002) HLA-B27 subtypes differentially associated with disease exhibit subtle structural alterations. J Biol Chem 277:47844–47853

Hülsmeyer M, Fiorillo MT, Bettosini F, Sorrentino R, Saenger W, Ziegler A, Uchanska-Ziegler B (2004) Dual, HLA-B27 subtype-dependent conformation of a self-peptide. J Exp Med 199:271–281

Hülsmeyer M, Welfle K, Pöhlmann T, Misselwitz R, Alexiev U, Welfle H, Saenger W, Uchanska-Ziegler B, Ziegler A (2005) Thermodynamic and structural equivalence of two HLA-B27 subtypes complexed with a self-peptide. J Mol Biol 346:1367–1379

Insaidoo FK, Zajicek J, Baker BM (2009) A general and efficient approach for NMR studies of peptide dynamics in class I MHC peptide binding grooves. Biochemistry 48:9708–9710

Kjer-Nielsen L, Clements CS, Purcell AW, Brooks AG, Whisstock JC, Burrows SR, McCluskey J, Rossjohn J (2003) A structural basis for the selection of dominant alphabeta T cell receptors in antiviral immunity. Immunity 18:53–64

Kumar P, Vahedi-Faridi A, Saenger W, Ziegler A, Uchanska-Ziegler B (2009) Conformational changes within the HLA-A1:MAGE-A1 complex induced by binding of a recombinant antibody fragment with TCR-like specificity. Protein Sci 18:37–49

Kushner DJ, Baker A, Dunstall TG (1999) Pharmacological uses and perspectives of heavy water and deuterated compounds. Can J Physiol Pharmacol 77:79–88

Leiting B, Marsilio F, O'Connell JF (1998) Predictable deuteration of recombinant proteins expressed in *Escherichia coli*. Anal Biochem 265:351–355

MacFerrin KD, Terranova MP, Schreiber SL, Verdine GL (1990) Overproduction and dissection of proteins by the expression-cassette polymerase chain reaction. Proc Natl Acad Sci USA 87:1937–1941

Madden DR (1995) The three-dimensional structure of peptide–MHC complexes. Annu Rev Immunol 13:587–622

Madden DR, Gorga JC, Strominger JL, Wiley DC (1992) The three-dimensional structure of HLA-B27 at 2.1 A resolution suggests a general mechanism for tight peptide binding to MHC. Cell 70:1035–1048

Marley J, Lu M, Bracken C (2001) A method for efficient isotopic labeling of recombinant proteins. J Biomol NMR 20:71–75

Michielin O, Karplus M (2002) Binding free energy differences in a TCR–peptide–MHC complex induced by a peptide mutation: a simulation analysis. J Mol Biol 324:547–569

Mittermaier A, Kay LE (2006) New tools provide new insights in NMR studies of protein dynamics. Science 312:224–228

Mittermaier AK, Kay LE (2009) Observing biological dynamics at atomic resolution using NMR. Trends Biochem Sci 34:601–611

Narzi D, Becker CM, Fiorillo MT, Uchanska-Ziegler B, Ziegler A, Böckmann RA (2012) Dynamical characterization of two differentially disease associated MHC class I proteins in complex with viral and self-peptides. J Mol Biol 415:429–442

Okon M, Bray P, Vucelic D (1992) 1H NMR assignments and secondary structure of human beta 2-microglobulin in solution. Biochemistry 31:8906–8915

Paliy O, Bloor D, Brockwell D, Gilbert P, Barber J (2003) Improved methods of cultivation and production of deuteriated proteins from *E. coli* strains grown on fully deuteriated minimal medium. J Appl Microbiol 94:580–586

Pervushin K, Riek R, Wider G, Wüthrich K (1997) Attenuated T2 relaxation by mutual cancellation of dipole-dipole coupling and chemical shift anisotropy indicates an avenue to NMR structures of very large biological macromolecules in solution. Proc Natl Acad Sci USA 94:12366–12371

Pöhlmann T, Böckmann RA, Grubmüller H, Uchanska-Ziegler B, Ziegler A, Alexiev U (2004) Differential peptide dynamics is linked to major histocompatibility complex polymorphism. J Biol Chem 279:28197–28201

Reche PA, Reinherz EL (2003) Sequence variability analysis of human class I and class II MHC molecules: functional and structural correlates of amino acid polymorphisms. J Mol Biol 331:623–641

Reiser JB, Darnault C, Gregoire C, Mosser T, Mazza G, Kearney A, van der Merwe PA, Fontecilla-Camps JC, Housset D, Malissen B (2003) CDR3 loop flexibility contributes to the degeneracy of TCR recognition. Nat Immunol 4:241–247

Reveille JD (2012) Genetics of spondyloarthritis—beyond the MHC. Nat Rev Rheumatol 8:296–304

Röben M, Hahn J, Klein E, Lamparter T, Psakis G, Hughes J, Schmieder P (2010) NMR spectroscopic investigation of mobility and hydrogen bonding of the chromophore in the binding pocket of phytochrome proteins. Chemphyschem: a European journal of chemical physics and physical chemistry 11: 1248–1257

Rognan D, Scapozza L, Folkers G, Daser A (1994) Molecular dynamics simulation of MHC–peptide complexes as a tool for predicting potential T cell epitopes. Biochemistry 33:11476–11485

Rückert C, Fiorillo MT, Loll B, Moretti R, Biesiadka J, Saenger W, Ziegler A, Sorrentino R, Uchanska-Ziegler B (2006) Conformational dimorphism of self-peptides and molecular mimicry in a disease-associated HLA-B27 subtype. J Biol Chem 281:2306–2316

Rudolph MG, Stanfield RL, Wilson IA (2006) How TCRs bind MHCs, peptides, and coreceptors. Annu Rev Immunol 24:419–466

Shi Y, Qi J, Iwamoto A, Gao GF (2011) Plasticity of human CD8alphaalpha binding to peptide-HLA-A*2402. Mol Immunol 48:2198–2202

Taurog JD (2009) Animal models of spondyloarthritis. Adv Exp Med Biol 649:245–254

Tugarinov V, Hwang PM, Kay LE (2004) Nuclear magnetic resonance spectroscopy of high-molecular-weight proteins. Annu Rev Biochem 73:107–146

Uchanska-Ziegler B, Ziegler A, Schmieder P (2013) Structural and dynamic features of HLA-B27 subtypes. Curr Opin Rheumatol 25:411–418

Varani L, Bankovich AJ, Liu CW, Colf LA, Jones LL, Kranz DM, Puglisi JD, Garcia KC (2007) Solution mapping of T cell receptor docking footprints on peptide–MHC. Proc Natl Acad Sci USA 104:13080–13085

Vranken WF, Boucher W, Stevens TJ, Fogh RH, Pajon A, Llinas M, Ulrich EL, Markley JL, Ionides J, Laue ED (2005) The CCPN data model for NMR spectroscopy: development of a software pipeline. Proteins 59:687–696

Wan S, Coveney P, Flower DR (2004) Large-scale molecular dynamics simulations of HLA-A*0201 complexed with a tumor-specific antigenic peptide: can the alpha3 and beta2 m domains be neglected? J Comput Chem 25:1803–1813

Winkler K, Winter A, Rueckert C, Uchanska-Ziegler B, Alexiev U (2007) Natural MHC class I polymorphism controls the pathway of peptide dissociation from HLA-B27 complexes. Biophys J 93:2743–2755

Yin Y, Mariuzza RA (2009) The multiple mechanisms of T cell receptor cross-reactivity. Immunity 31:849–851

Zacharias M, Springer S (2004) Conformational flexibility of the MHC class I alpha1–alpha2 domain in peptide bound and free states: a molecular dynamics simulation study. Biophys J 87:2203–2214

Zhu J, Rao H, Tonelli M, Westler WM, Singarapu KK, Markley JL, DeLuca HF, Assadi-Porter FM (2012) Efficient stable isotope labeling and purification of vitamin D receptor from inclusion bodies. Protein Expression Purif 85:25–31

Ziegler A, Loll B, Misselwitz R, Uchanska-Ziegler B (2009) Implications of structural and thermodynamic studies of HLA-B27 subtypes exhibiting differential association with ankylosing spondylitis. Adv Exp Med Biol 649:177–195